Fracture toughness of steel adherend bonded with two-part polyurethane adhesives: Double cantilever beam tests under static loading

Yuki Ogawa[a,1,*], Kimiyoshi Naito[a], Keisuke Harada[a,2] and Hiroyuki Oguma[a]

[a] Polymer Matrix Hybrid Composite Materials Group, Research Center for Structural Materials, National Institute of Materials Science, 1-2-1 Sengen, Tsukuba, Ibaraki, Japan

[1] Now at Department of Mechanical Engineering, Graduate School of Engineering, Kobe University, 1-1 Rokkodai-cho, Nada-ku, Kobe, Hyogo, 657-8501, Japan

[2] Now at Naval Platform and Signature Technology Division, Naval Systems Research Center, Acquisition, Technology & Logistics Agency, 2-2-1 Nakameguro, Meguro-ku, Tokyo, 153-8630, Japan.

[*] Correspondence author

TEL: +81 78-803-6128

FAX: +81 78-803-6321

Email: yogawa@mech.kobe-u.ac.jp

NOMENCLATURE

a : apparent crack length

A_1,A_2 : constant of linear relation of a cube root of compliance and apparent crack length

B : width of DCB specimen

C : compliance

$\sqrt[3]{C}$: cube root of the compliance

G_I : energy release rate

G_{IC} : fracture toughness

P : load

P_{arr} : arrest load

P_{ine} : inelastic load

P_{max} : maximum load

δ : displacement

ε : strain

σ : stress

ABSTRACT

The ductile structural adhesives such as a polyurethane adhesive are developed in recent years. This study is intended to measure the fracture toughness under Mode I loading of two-part polyurethane adhesives using double cantilever beam (DCB) tests. Two types of polyurethane adhesives and the effect of adhesive thickness on the fracture toughness are discussed. Plastic deformation of the steel adherends occurred in both adhesives for both adhesive types and thicknesses. Therefore, the arrest load out of consideration of a plastic deformation was evaluated the fracture toughness of the DCB specimens. As a result, the fracture toughness of the polyurethane adhesive is higher for higher tensile modulus and adhesive strength. In addition, the fracture toughness is higher for a larger adhesive thickness. The analytical results based on the triangle cohesive zone model using zero-thickness cohesive elements are agreed with the experimental results.

***Keywords*:** Adhesive joints, Fracture toughness, Crack, Cohesive zone

1. INTRODUCTION

Adhesive bonding leads to weight reduction, high rigidity, and air tightness for aerospace and automobile structures because it is a surface bonding technique and can

distribute the stress at a joint[1,2]. Structural adhesives were developed and applied in industrial fields other than welding and riveting[3]. Structural adhesives require high performance, heat resistance, and corrosion resistance. Therefore, adhesives composed of thermosetting resins were mainly applied. Epoxy adhesives are high-strength and functional adhesives and have been applied in actual transportation[4,5]. However, epoxy adhesives were prone to brittle fracture. In order to prevent the brittle fracture in the bonded structures, ductile structural adhesives were developed in recent years[6,7]. A polyurethane adhesive, which is a ductile adhesive, has a high fracture toughness because polyurethane adhesives can be designed with a wide range of setup characteristics[8-10]. However, the durability and reliability of bonded structures with ductile adhesives were lower than those of welded structures, so that the design basis of adhesive bonding was uncertain.

Studies on a failure criterion based on the fracture mechanisms of adhesive have been widely conducted. The strength of adhesive bonded joints predicted from the traction-separation law used a cohesive zone model in each of Modes I, II, and III[11-14]. In the case of Mode I, double cantilever beam (DCB) tests can simply measure the energy release rate of the adhesives based on beam theory. Although DCB tests have been carried out for many adhesives[15,16], there are few reports of polyurethane adhesives in Mode I loading compared to other adhesives[17,18]. It is necessary to clarify the energy release rate and the fracture mechanism under Mode I loading for a wide range of polyurethane adhesives. Moreover, research on the optimal condition of adhesive bonded joints remains insufficient. In order to establish the design basis of adhesive bonding, comprehensive knowledge of adhesive bonding structures must be investigated.

The present study examined the fracture toughness and fracture behavior under Mode I loading of steel adherends bonded with two types of polyurethane adhesives by

DCB tests. The effect of adhesive thickness[19,20], which is one of the factors governing the joint strength of adhesive bonding, on the fracture toughness is also discussed.

2. EXPERIMENTAL PROCEDURES

2.1. Materials

A carbon steel sheet based on JIS G3101 SS400 was used as the adherend. Two commercially available types of two-part polyurethane adhesives, BETAFORCE™ 2850L and BETAFORCE™ 9050L, both produced by DuPont, were used. We refer to these two adhesive types as *2850L* and *9050L*, respectively.

2.2. Specimens

In order to determine the material properties of both adhesives, tensile tests were carried out on dog-bone-type specimens based on JIS K 6251 No. 8[21], as shown in Figure 1.

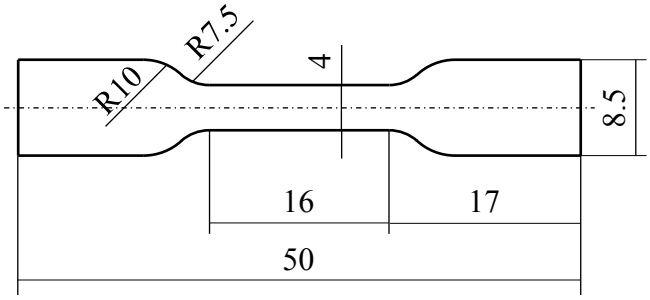

FIGURE 1 Shape and dimension of the dog-bone type specimen (unit: mm).

Figure 2 shows the shape and dimensions of the DCB specimen based on JIS K 7086[22]. The steel adherends were sandblasted with brown fused alumina abrasives and were degreased by acetone. A primer, Hamatite Body Primer, supplied by Yokohama Rubber Co. Ltd., was applied to the steel adherends before the adhesive bonding. A high-

performance fluoropolymer-release film, WL5200, with a thickness of 25 μm was used to create an initial crack with a length of approximately 40 mm. In order to investigate the effects of adhesive thickness, *t*, under Mode I loading, two adhesion thicknesses of 3.0 and 0.3 mm were produced by spacer stainless sheets. They were kept at room temperature for 3 days, and then heated up to 80°C for 24 hours in an oven. After curing, the adhesive thickness of the DCB specimen was measured using a digital microscope.

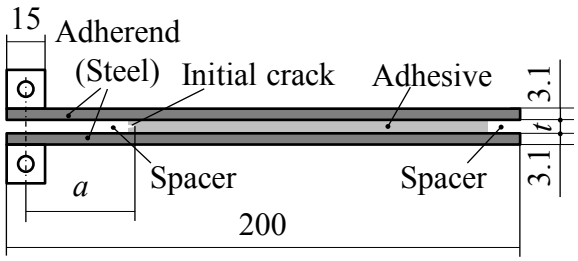

FIGURE 2 Shape and dimensions of the double cantilever beam (DCB) specimen (units: mm).

2.3. Testing conditions

Tensile tests for the dog-bone-type specimens were conducted under displacement control at a crosshead speed of 1.0 mm min^{-1}. The elongation at breaking was measured by a non-contact video extensometer. At least three specimens were tested for both adhesives.

Double cantilever beam tests were conducted using a tensile test machine under displacement control at a crosshead speed of 1.0 mm min^{-1}. In order to introduce an artificial crack, the DCB specimen was loaded until the crack length reached approximately 70 mm in the case of an adhesive thickness of 0.3 mm, or 50 mm in the case of an adhesive thickness of 3.0 mm. The initial load-displacement curve was not used to measure the energy release rate. Figure 3 shows a diagram of the DCB test used herein.

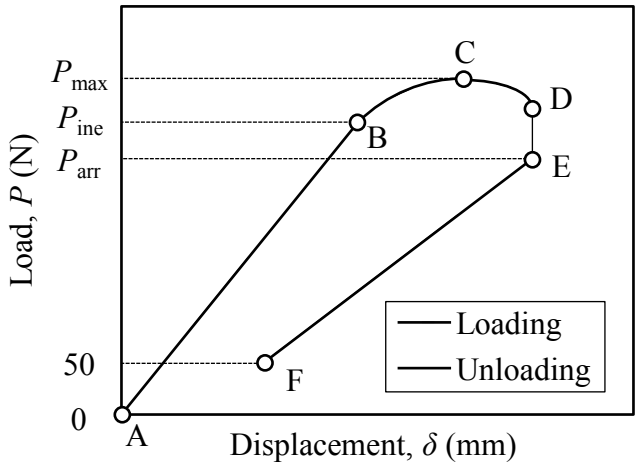

FIGURE 3 Diagram of the DCB test method used herein.

The DCB specimen was loaded until the crack grew to a length of approximately 5 mm. The load-displacement curve (P-δ curve) was linear from point A to point B in the figure, and the crack had not yet propagated. When nonlinearity appeared in the load-displacement curve from point B to point C in the figure, the crack gradually propagated. The load at point B is referred to the inelastic load, P_{ine}. After reaching the maximum load, P_{max}, at point C, the displacement increased until the crack propagated approximately 5 mm (point D). In order to stop crack propagation, the DCB test was paused for approximately 30 minutes. The load when the DCB test was restarted (point E) was defined as the arrest load, P_{arr}. In the case of ductile adhesives, plastic deformation occurred in the thin steel adherends of the DCB specimen, as described later. Therefore, the crack length in the DCB tests was defined as the linear difference between load points and the crack tip by measurement using a microscope. This distance is referred as the apparent crack length, a. Then, the DCB specimen was unloaded to 50 N and then re-loaded, as shown by points E–F–E in the figure. Such loading and unloading cycles were performed until the DCB

specimen completely failed, and the energy release rate was calculated for each cycle. At least three specimens were investigated for both adhesives and both adhesive thicknesses.

3. RESULTS

3.1. Stress-strain curves for each adhesive

Figure 4 shows the stress-strain curves (σ-ε curves) for the adhesive bulk specimens. Both adhesives show highly nonlinear behavior. Table 1 shows the tensile test results for both polyurethane adhesives. The tensile modulus and strength for the *9050L* adhesive was higher than those for the *2850L* adhesive. In contrast, the strain at failure for the *2850L* adhesive was higher than that for the *9050L* adhesive.

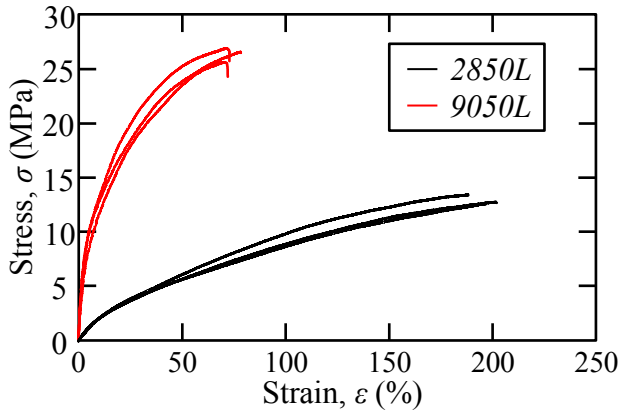

FIGURE 4 Stress-strain curves for both polyurethane adhesives.

TABLE 1 Mechanical properties of each polyurethane adhesive.

Adhesive	Tensile strength (MPa)	Strain at failure (%)
2850L	12.9	196.0
9050L	26.3	74.7

3.2. Double cantilever beam test results

Figure 5 shows the load-displacement curves obtained in the DCB tests. Both adhesives exhibited inelastic behavior. In addition, the load decreased and the crack propagated before restarting the test in one cycle. The results for the side of the specimen for each adhesive before restarting the tests are shown in Figure 6. Plastic deformation of the steel adherends occurred in both adhesives for both adhesive types and thicknesses, and a residual displacement was also observed in the load-displacement curves. It is necessary to establish evaluation methods for the fracture toughness in the case where the adherend experiences plastic deformation.

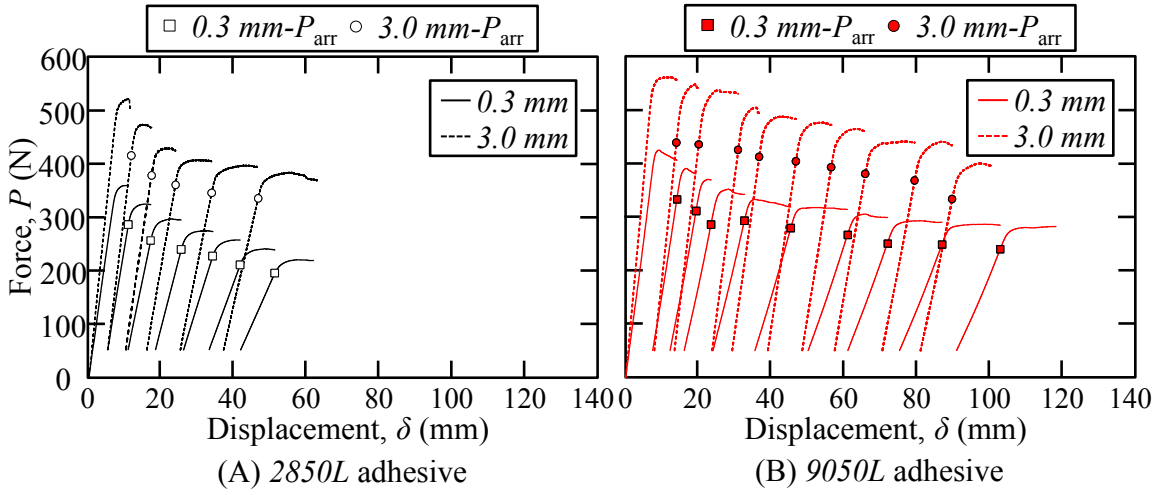

FIGURE 5 Load–displacement curves during DCB tests.

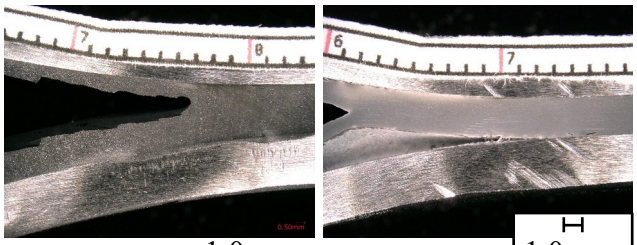

(A) *2850L* adhesive (B) *9050L* adhesive

FIGURE 6 Observation results for the side of the DCB specimens just before restarting the tests.

The energy release rate for adhesives was calculated from the relationship between the compliance and apparent crack length. Figure 7 shows the relationship between the cube root of the compliance and the apparent crack length. This relationship was linear for all adhesives and adhesive thicknesses. When this relation is defined by equation (1), the relationship between the compliance and the apparent crack length is expressed by the cubic formula shown in equation (2). The energy release rate, G_I, is calculated using equation (3), where B is the width of the DCB specimen. It is considered that the inelastic load, P_{ine}, and the maximum load, P_{max}, include the effect of plastic deformation of the steel adherends. Moreover, the energy release rate, which was calculated based on these loads, was overestimated, and the evaluation of the fracture toughness was not suitable. Therefore, the arrest load, P_{arr}, which was not affected by plastic deformation of the steel adherends, was used to evaluate the fracture toughness, G_{IC}, of the DCB specimens.

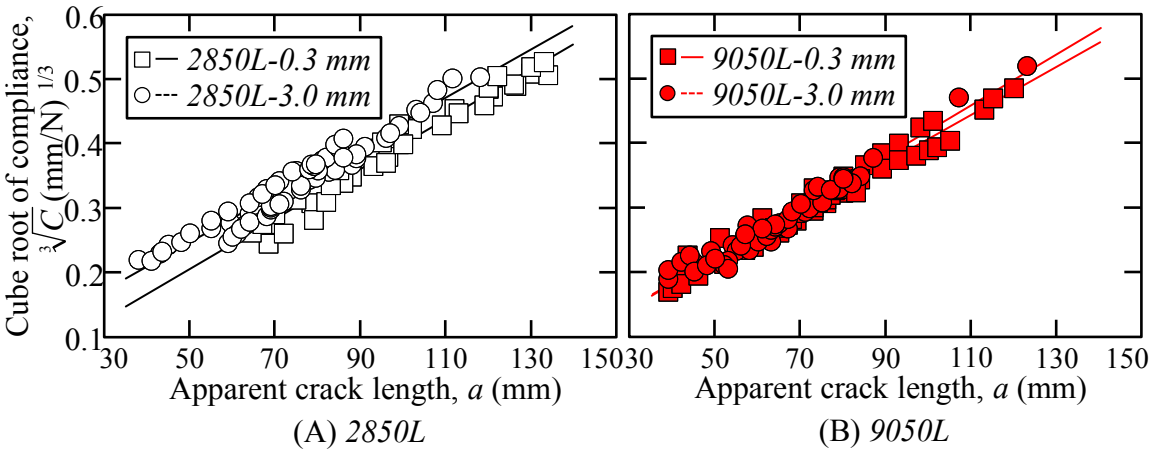

FIGURE 7 Relationship between the cube root of compliance and the apparent crack length.

$$\sqrt[3]{C} = A_1 a + A_2 \tag{1}$$

$$C = A_1^3 a^3 + 3A_1^2 A_2 a^2 + 3A_1 A_2^2 a + A_2^3 \tag{2}$$

$$G_I = \frac{P^2}{2B}\frac{dc}{da} = \frac{P^2}{2B}\left(3A_1^3 a^2 + 6A_1^2 A_2 a + 3A_1 A_2^2\right) \tag{3}$$

Figure 8 shows the relationships between the fracture toughness and the apparent crack length for all DCB tests. The fracture toughness showed similar values in the region in which the crack propagated stably, regardless of the difference in the adhesive and the adhesive thickness. The lines in Figure 8 and the entries in Table 2 show the average values of the fracture toughness for each adhesive thickness for both polyurethane adhesives. The fracture toughness of the polyurethane adhesive is higher for a higher tensile modulus and higher adhesive strength. In addition, the fracture toughness is higher for a larger adhesive thickness.

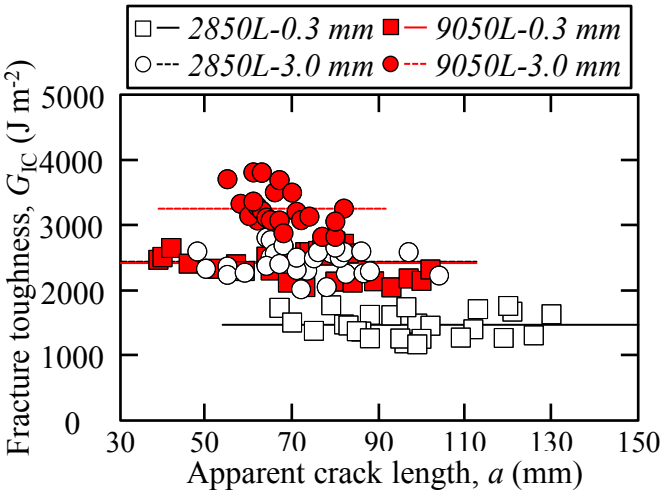

FIGURE 8 Relationship between fracture toughness and apparent crack length.

TABLE 2 Average values of fracture toughness for each adhesive thickness for both adhesives

Adhesive	Fracture toughness, G_{IC} (J m^{-2})	
	t=0.3 mm	*t=3.0 mm*
2850L	1466	2436
9050L	2414	3255

The morphologies of the fracture surfaces were observed for each DCB specimen. Figure 9 shows representative fracture surfaces. The left-hand side of the figure shows overall views of the fracture surface, and enlarged images of the regions outlined in red are shown on the right-hand side of the figure. In the case of the fracture surfaces of the *2850L* adhesive, the adhesive partially adhered to the steel adherends. Therefore, this adhesive fractured by both interfacial failure and cohesive failure. However, the *9050L* adhesive underwent mainly cohesive failure under Mode I loading. In general, cohesive failure tends to increase with increasing fracture toughness[23], so the fracture toughness is assumed to be

higher for the high-tensile-strength adhesive. Another factor is that irregularities on the fracture surface and the crack propagation resistance for the *9050L* adhesive increased for larger fracture surfaces. This has been evaluated based on the fractal dimension, and the fractal dimension and the fracture toughness increase as the content of rubber in the adhesive increases[23,24]. These points require more detailed examination, including investigation of the bulk properties, and will be considered in future studies.

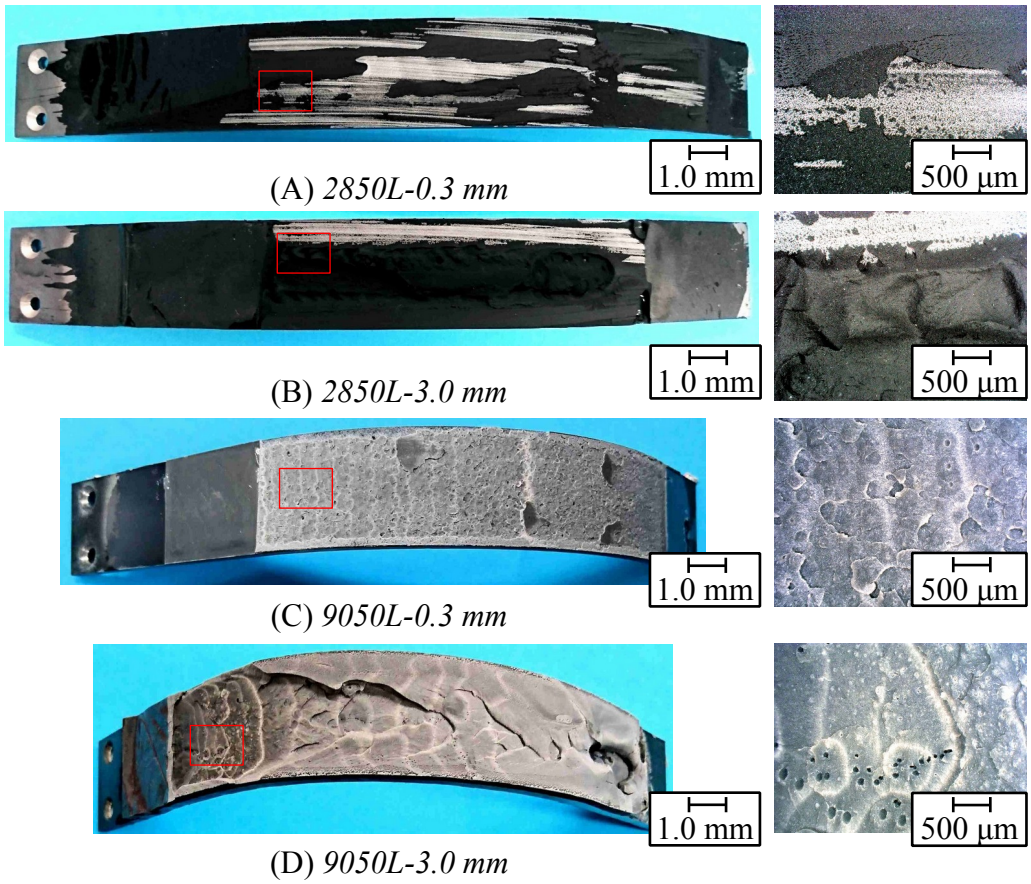

FIGURE 9 Fracture surfaces of the DCB specimens.

3.3. Finite element method analysis

In order to evaluate the fracture toughness of polyurethane adhesives based on the cohesive zone model, the finite element method (FEM) analysis with ABAQUS was used in the present study. Figure 10 shows the analysis model for the DCB specimen in the case of an adhesive thickness of 1.0 mm. A linear analysis in a plane strain state was applied. The analysis model was a half model formed by isoparametric quadrilateral elements. The material properties for the adherend were for an elastic material, and those for the adhesives were for hyperelastic materials in the Arruda-Boyce model. The parameters for the Arruda-Boyce model were estimated based on the tensile test results, as shown in Figure 4. The FEM analysis was performed for four adhesive thicknesses of 0.1, 0.3, 1.0, and 3.0 mm using the triangle cohesive zone model. Table 3 shows the number of elements and nodes for each adhesive thickness. The cohesive fracture toughness was used to estimate the fracture toughness in the case of zero adhesive thickness based on the relationship between the fracture toughness and the adhesive thickness in the DCB tests, as shown in Figure 11. The cohesive fracture toughness is 1,358 J m^{-2} for the *2850L* adhesives and 2,321 J m^{-2} for the *9050L* adhesives. Thus, FEM analysis was conducted in order to evaluate the failure behavior of polyurethane adhesives using the parameters for the adhesives and the zero-thickness cohesive elements[25,26].

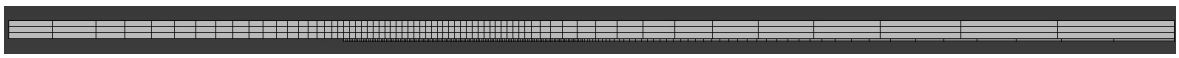

FIGURE 10 Analysis model for DCB specimen.

TABLE 3 Analysis parameters of each adhesive joint

Adhesive thickness	Elements	Nodes
0.1 mm	735	480
0.3 mm	919	662
1.0 mm	919	662
3.0 mm	948	660

Figure 11 also shows the analytical results for the fracture toughness and the adhesive thickness. The analytical results agree with the experimental results. The analysis based on the triangle cohesive zone model using zero-thickness cohesive elements could be used to evaluate the fracture toughness of both polyurethane adhesives with different adhesive thicknesses. The fracture toughness of the ductile adhesives in steel adherends could be evaluated based on the arrest load out of consideration of a plastic deformation.

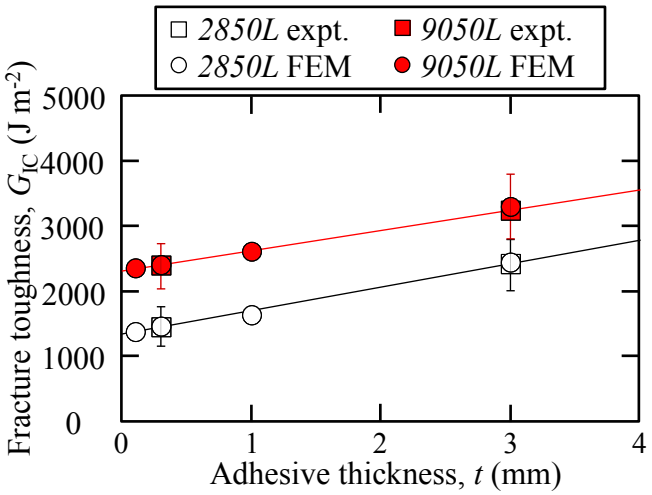

FIGURE 11 Experimental and analytical results. Relationship between fracture toughness and adhesive thickness.

4. CONCLUSION

Double cantilever beam tests were conducted in order to measure the fracture toughness under Mode I loading in steel adherends bonded with two types of two-part polyurethane adhesives, i.e., BETAFORCE™ 2850L and BETAFORCE™ 9050L. The effect of adhesive thickness for both adhesive types was also investigated. The fracture toughness, which was evaluated based on the arrest load in the DCB tests, for BETAFORCE™ 2850L was 1,466 J m^{-2} for a thickness of 0.3 mm and 2,436 J m^{-2} for a thickness of 3.0 mm. In the case of BETAFORCE™ 9050L, the fracture toughness was 2,414 J m^{-2} for a thickness of 0.3 mm and 3,255 J m^{-2} for a thickness of 3.0 mm. The fracture toughness of the *9050L* adhesive was higher than that of the *2850L* adhesive, and the fracture toughness of thick adhesive was higher than that of thin adhesive. These experimental results agreed with the analytical results based on the triangle cohesive zone model using zero-thickness cohesive elements.

Acknowledgements

This paper is based on results obtained from a future pioneering project commissioned by the New Energy and Industrial Technology Development Organization (NEDO).

References

1. Barnes TA, Pashby IR. Joining techniques for aluminium spaceframes used in automobiles: Part II - adhesive bonding and mechanical fasteners. *J Mater Process Technol*. 2000;99:72-79.
2. Higgins A. Adhesive bonding of aircraft structures. *Int J Adhes Adhes*. 2000;20(5):367-376.

3. Baldan A. Adhesively-bonded joints and repairs in metallic alloys, polymers and composite materials: Adhesives, adhesion theories and surface pretreatment. *J. Mater. Sci*. 2004;39:1-49.
4. Grant LDR, Adams RD, da Silva LFM. Experimental and numerical analysis of single-lap joints for the automotive industry. *Int J Adhes Adhes*. 2009;29(4):405-413.
5. Rohde BJ, Le KM, Krishnamoorti R, Robertson ML. Thermoset Blends of an Epoxy Resin and Polydicyclopentadiene. *Macromolecules*. 2016;49:8960-8970.
6. Angelidi M, Vassilopoulos AP. Keller T. Displacement rate and structural effects on Poisson ratio of a ductile structural adhesive in tension and compression. *Int J Adhes Adhes*. 2017;78:13-22.
7. Galvez P, Abenojar J, Martinez MA. Effect of moisture and temperature on the thermal and mechanical properties of a ductile epoxy adhesive for use in steel structures reinforced with CFRP. *Compos. B. Eng*. 2019;176:107194.
8. Xiao Y, Stuedlein AW, Chen Q, Liu H, Liu P. Stress-Strain-Strength Response and Ductility of Gravels Improved by Polyurethane Foam Adhesive. *J. Geotech. Geoenviron. Eng*. 2018;144(2):04017108.
9. Banea MD, da Silva LFM, Campilho RDSG. The Effect of Adhesive Thickness on the Mechanical Behavior of a Structural Polyurethane Adhesive. *J Adhes*. 2015;91(5): 331-346.
10. Jia Z, Yuan G, Feng X, Zou Y, Yu J. Shear properties of polyurethane ductile adhesive at low temperatures under high strain rate conditions. *Compos. B. Eng*. 2019;156(1):292-302.
11. Elices M, Guinea GV, Gómez J, Planas J. The cohesive zone model: advantages, limitations and challenges. *Eng Fract Mech*. 2002;69(2):137-163.

12. Zaeri AR, Googarchin HS. Analysis of automotive mixed−adhesive joints weakened by moist conditions: Experimental characterization and numerical simulation using cohesive zone model. *Fatigue Fract Eng Mater Struct*. 2019;42:929-942.
13. Delbariani-Nejad A, Malakouti M, Farrokhabadi A. Reliability analysis of metal−composite adhesive joints under debonding modes I, II, and I/II using the results of experimental and FEM analyses. *Fatigue Fract Eng Mater Struct*. 2019;42:2644-2662.
14. Ramalho LDC, Campilho RDSG, Belinha J, da Silva LFM. Static strength prediction of adhesive joints: A review. *Int J Adhes Adhes*. 2020;96:102451.
15. Ashcroft IA, Hughes DJ, Shaw SJ. Mode I fracture of epoxy bonded composite joints: 1. Quasi-static loading. *Int J Adhes Adhes*. 2001;21(2):87-99.
16. Kim HB, Naito K, Oguma H. Double cantilever-beam test comparisons of Mode I fracture toughness of adherends bonded using DP8010 and DP8005 acrylic-based adhesives. *Int J Adhes Adhes*. 2018;82:173-183.
17. Gálvez P, Carbas RJC, Campilho RDSG, Abenojar J, Martínez MA, da Silva LFM. Fracture toughness in Mode I (G_{IC}) for ductile adhesives. *J Phys Conf Ser*. 2017;843:012008.
18. Faneco T, Campilho R, Silva F, Lopes R. Strength and Fracture Characterization of a Novel Polyurethane Adhesive for the Automotive Industry. *J Test Eval*. 2017;45(2):398-407.
19. Naito K, Onta M, Kogo Y. The effect of adhesive thickness on tensile and shear strength of polyimide adhesive. *Int J Adhes Adhes*. 2012;36:77-85.
20. Marzi S, Biel A, Stigh U. On experimental methods to investigate the effect of layer thickness on the fracture behavior of adhesively bonded joints. International Journal of Adhesion and Adhesives. *Int J Adhes Adhes*. 2011;31(8):840-850.
21. Rubber, vulcanized or thermoplastics - determination of tensile stress–strain properties, JIS K 6251.

22. Testing methods for interlaminar fracture toughness of carbon fibre reinforced plastics, JIS K 7086.
23. Naito K, Fujii T. Static and fatigue crack growth of epoxy adhesives and fractal dimensions. *Int J Adhes Adhes*. 1998;18(3):199-213.
24. Naito K, Fujii T. Fractals for fractured surfaces of adhesives under static and fatigue loadings. *Int J Adhes Adhes*. 1995;15(3):123-130.
25. Luo Q, Tong L. Fracture Prediction of Adhesively Bonded Structures Using Energy Release Rates. *J Adhes Sci Technol*. 2009;23(10-11):1415-1440.
26. Dimitri R, Cornetti P, Manti V, Trullo M, De Lorenzis L. Mode-I debonding of a double cantilever beam: A comparison between cohesive crack modeling and Finite Fracture Mechanics. *Int J Solids Struct*. 2017;124:57-72.